Experiments with "doubly"-spin-polarized atomic hydrogen

R. Sprik, J. T. M. Walraven, and G. H. van Yperen*
Natuurkundig Laboratorium, Universiteit van Amsterdam, Valckenierstraat 65, 1018 XE Amsterdam, The Netherlands

Isaac F. Silvera
Lyman Laboratory of Physics, Harvard University, Cambridge, Massachusetts 02138
(Received 7 April 1986)

We analyze and reinterpret experiments with electron- and nuclear-spin ("doubly")-polarized hydrogen (H↓↓) in a cell with a very low concentration of magnetic impurities. The destabilizing magnetic relaxation due to remaining impurities (G_i^s) is found to be suppressed by increasing the thickness of the helium film covering the walls of the cell. Using recent information on surface three-body recombination, we obtain good quantitative agreement with more recent experiments if we assume thermal gradients, up to $\Delta T/T \simeq 0.1$. We extract both the value and field dependence for the three-body surface recombination [$L_3^s = 1.5(2) \times 10^{-24}$ cm^{4}s^{-1} at $B = 8$ T]. We also extract the magnetic field dependence of the impurity relaxation.

I. INTRODUCTION

The gaseous state of atomic hydrogen (H) has been studied extensively at low temperatures ($T = 60$ mK–1 K) in liquid-helium-covered sample cells.[1–4] By polarizing the electronic spins (H↓) in a high magnetic field ($B \simeq 10$ T) densities in the range $n = 10^{16}$–10^{17} cm^{-3} were achieved. Still higher densities up to 4.5×10^{18} cm^{-3} were reported for samples in which both the electronic and nuclear spins were polarized (H↓↓). Nevertheless these densities are not sufficiently high to observe the transition to the Bose-Einstein condensed phase, predicted at

$$n_c = (mk_B T_c / 3.31\hbar^2)^{3/2} \simeq 1.6 \times 10^{19} \text{ cm}^{-3}$$

for $T_c = 100$ mK. In this paper we discuss experiments with a cell void of magnetic impurities in which we studied H↓↓ and address some of the limitations to reach high densities. The results were published earlier as a short report[5] (further referred to as I).

The barrier to achieving high densities of atomic hydrogen is recombination to H_2 which must take place by three-body collisions involving two or three H atoms. Although electron-spin polarization strongly reduces the recombination probability, H↓ has been found to recombine at a rate proportional to n^2 (with He surface atoms participating as "third bodies"). The maximum density that can be built up by continuously filling the cell is then limited to $n \simeq 10^{16}$–10^{17} cm^{-3}. The main recombination processes between atoms in the two lower hyperfine states (H↓) are driven by the admixture of electron spin ↑. These hyperfine states are the mixed state $|a\rangle = |{\downarrow\downarrow}\rangle - \epsilon|{\uparrow\downarrow}\rangle$ and the pure state $|b\rangle = |{\downarrow\downarrow}\rangle$, where $\epsilon = a/(4\mu_B B)$. Here a is the hyperfine mixing constant and μ_B the Bohr magneton; ↑ indicates electron-spin projection of $\frac{1}{2}$ and ↓, nuclear-spin projection of $\frac{1}{2}$ (the hyperfine states are labeled a, b, c, and d with increasing energy[1–4]). As described by Statt and Berlinsky[6] the absence of the admixture in the b state favors recombination of a-a and a-b pairs and leads to a rapid depletion of the a state, thus leaving a residual gas of only b-state atoms: the doubly-polarized state H↓↓. Since b-state atoms are in pure electron-spin-polarized states, they do not recombine by the second-order process (n_b^2) with He third bodies; as a consequence the stability of H↓↓ depends on the magnetic relaxation from the b state to the mixed hyperfine states $|a\rangle$ or $|c\rangle$. Alternatively, as pointed out by Kagan *et al.*,[7,8] recombination may proceed directly, without the relaxational step, through a process involving three b-state hydrogen atoms and thus scaling as n_b^3.

The first successful observation of the double-polarization mechanism and the enhanced stability of the gas was made by Cline *et al.*[9] The recombination times were found to be orders of magnitude longer than those found for H↓ and densities of 3×10^{17} cm^{-3} were achieved. Earlier experiments by van Yperen *et al.*[10] did not show a buildup of H↓↓, and high rates of recombination consistent with previous measurements[11–13] were observed. The fast recombination found by van Yperen *et al.* was attributed to rapid magnetic $b \rightarrow a$ relaxation induced by magnetic impurities in the wall of the sample cell. Once we recognized the role of magnetic impurities as an important source of relaxation we decided to construct a new cell, carefully avoiding all conspicuous magnetic materials.

The interpretation of the measurements by Cline *et al.*, I, and similar experiments by others,[14,15] was based on the model in which, at low temperature, surface relaxation followed by rapid recombination was assumed to be the dominant density decay mechanism. This interpretation led to a discrepancy of order 50 between experimental[5,9,14,15] and theoretical[16–19] values for the $b \rightarrow a$ surface relaxation rate constant G_{ab}^s.

With the development of techniques to compress a sample of H↓↓ to high density ($n > 10^{18}$ cm^{-3}),[20–24] measurements demonstrated the existence of the third-order recombination channels both in the bulk[20–24] and on the surface.[21–24] Hess *et al.*[22] realized that three-body sur-

face recombination also had been important in previous experiments at much lower bulk densities. This reinterpretation of the destabilization processes on the surface in terms of recombination instead of relaxation was recently confirmed by Reynolds *et al.*[25] using ESR techniques. At present, theory and experiment for G_{ab}^{s} agree well.[25] Discrepancies can be attributed to the unknown surface roughness of the cell walls.

In this paper we reexamine the results of I, extracting a value for the third-order surface recombination rate. A similar reanalysis of their earlier data has been given by Bell *et al.*[26] We also discuss how impurity relaxation may be suppressed by using thick ^{4}He films and extract the field dependence of both the three-body rate and the impurity relaxation. We find that no satisfactory theory is available to describe our results for third-order recombination. Bulk magnetic relaxation is found to be in agreement with other measurements[5,9,14,15] and theory.[6,16–19,27] In addition some technical details on the construction of the cell and the analysis of the decays are discussed.

II. EXPERIMENTAL CELL WITHOUT MAGNETIC IMPURITIES

The experimental cell is schematically shown in Fig. 1. The H is fed in from the bottom and observed with a pressure gauge, which is integrated into the body of the cell and placed in the center of an 11-T superconducting magnet. During operation all surfaces are covered with a film of liquid helium. The main sample volume has the pancake shape of the pressure gauge. The design combines a small volume, $V \simeq 5 \times 10^{-3}$ cm^3, with a large surface-to-volume ratio, $A/V \simeq 40$–140 cm^{-1}. The pancake shape implies that most surfaces in the cell are perpendicular to the direction of the main magnetic field. This may have consequences, as surface relaxation is predicted to be anisotropic as will be discussed in Sec. VI.

Before the actual design was made, all construction materials employed in the cell of van Yperen *et al.*[10] were carefully examined with respect to their magnetic properties. Chemical analysis of the oxygen-free high-conductivity (OFHC) copper to be used for the body of the cell showed that the concentration of magnetic impurities in the bulk of our OFHC copper is low (< 10 ppm).[28] Furthermore, to be effective as relaxation centers magnetic impurities have to be clustered since only magnetic fields due to sizable (ferro) magnetic grains (> 50 Å) range far enough to induce relaxation in the H↓ moving on top or near the helium film. The magnetic impurities observed in the chemical analysis may be diluted in the copper and are then harmless. A much more serious problem is the contamination of the copper surface caused by the machining of the copper. Chemical analysis of the first 0.5 μm of a machined piece of copper showed that the iron concentration in the top layer was 100 times larger than the bulk concentration. This indicated that one should etch off a layer of material after machining the copper with a magnetic tool bit, a procedure that was not performed in the construction of the cell of van Yperen *et al.* Some other materials used in the construction of that cell were investigated in a pendulum magnetometer between 1.6–300 K. Stycast 2850GT (catalyst 11) appeared to be ferromagnetic whereas Stycast 1266 was found to be diamagnetic to low temperatures (see also a recent publication[29]) and was used instead. Scotch no. 56 tape, a yellow mylar based tape used in the interior part of the cell of van Yperen *et al.*, was found to be slightly diamagnetic but was avoided in the new cell employing better attachment methods. Finally all copper electrical wires were stripped of their original possibly magnetic insulating varnishes and were reinsulated with Stycast 1266.

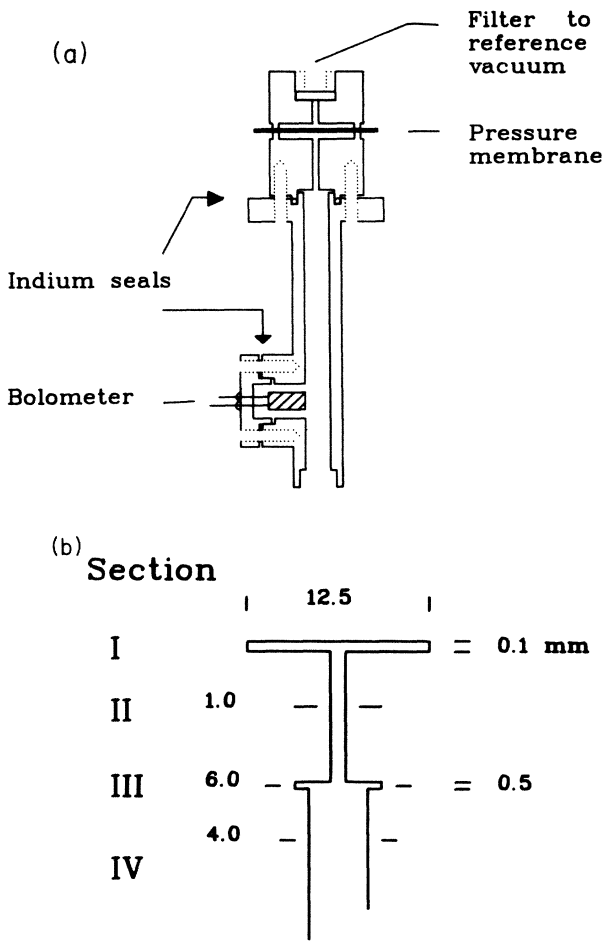

FIG. 1. Schematic overview of hydrogen stabilization cell, including the dimensions used to estimate the effective volumes and surfaces used in the analysis.

The construction of the membrane pressure gauge was done with great care to avoid contamination of the surfaces of the gauge. The evaporation of the gold layer on the Kapton membrane was done in a clean and simple evaporation apparatus, specially constructed for this purpose (see Fig. 2), using high-purity gold (99.999% pure). All copper parts in the heart of the cell were electrochemically etched in a solution of 60 vol. % H_3PO_4—40 vol. % H_2O using properly shaped Pt anodes. This etch technique allows a well-controlled removal of the contaminated top layer of the copper. (In later cells purely chemical

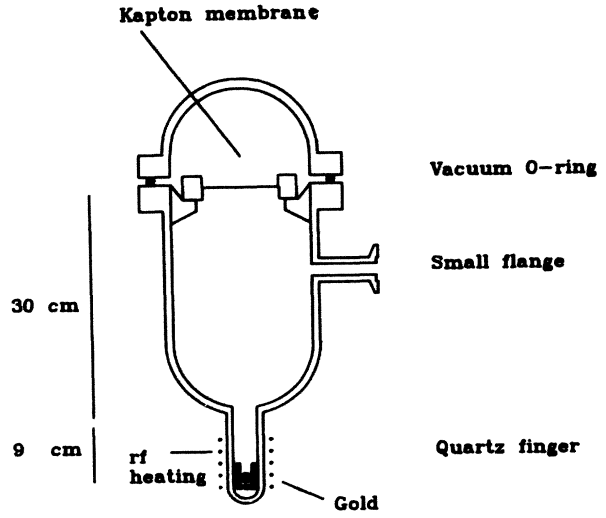

FIG. 2. Simple clean gold evaporation vacuum chamber.

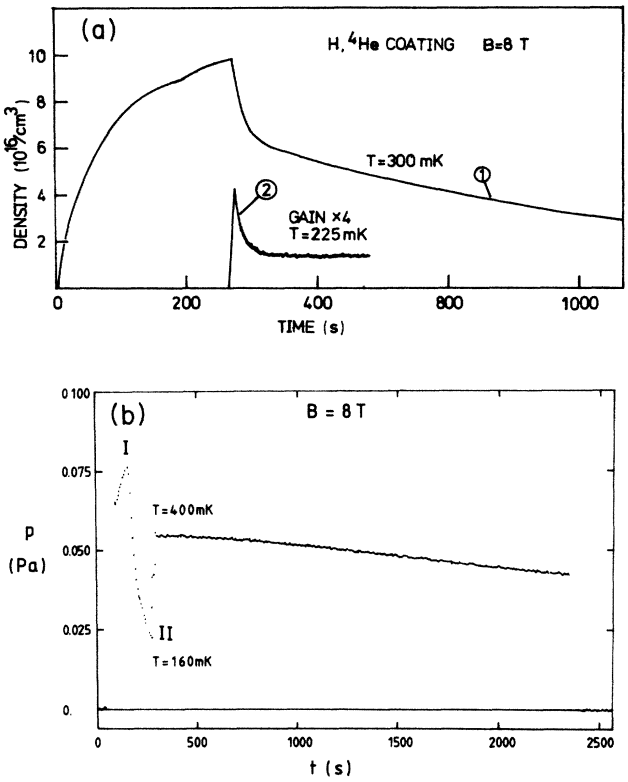

FIG. 3. (a) Building up of double polarization. ①—$T=300$ mK, high starting density, ②—$T=225$ mK, low starting density. (b) Decreased decay as a result of extra enhancement of the double polarization. At I the temperature is lowered rapidly from 400 to 160 mK and returns to 400 mK at II.

etching in HNO_3-H_2O acid was also used.) Instead of a carbon "trigger" bolometer with possible magnetic impurities a small solenoid of 10-μm tungsten wire on a Stycast 1266 rod was used (no magnetic impurities) and placed ~ 3 cm below the center of the magnet.

In contrast to one of our earlier cells, this one was void of sinter. As will be discussed later, this restricts the thermal contact between the helium and the copper cell body. The cell was connected to the same filling section as used by van Yperen *et al.*[10] and installed in an Oxford Instruments dilution refrigerator with bottom access. This part of the experimental setup is described in detail elsewhere.[15,30]

III. MEASUREMENTS

The recombination kinetics of the H gas was studied by measuring the pressure decay as a function of time. As an example we show in Fig. 3(a) a decay curve typical for 300 mK and 8 T. In the first part of the decay double polarization is building up, displaying itself as a rapid initial decay due to a-a and a-b recombination, followed by a much slower relaxation bottlenecked decay due to $b \rightarrow a$ relaxation in the gas phase. The rate constants characterizing the recombination (K_{aa} and K_{ab}) and relaxation (G_{ab} or G_{ab}^i) will be discussed in Sec. IV.

The final polarization depends on the relative efficiency of the relaxation processes by which the b state is depleted and the recombination processes that preferentially eliminate the a-state atoms.[6] This opens the possibility to prepare a sample in a condition where the a to b ratio is smaller than the equilibrium value at a given temperature. This is illustrated in Fig. 3(b). After filling the cell, a sample is first cooled to low temperature thus building up a high degree of polarization and subsequently rapidly warmed up again to the original temperature. The initial decay of the pressure is slowed down by this procedure until relaxation restores the equilibrium situation at that temperature. This qualitative proof of bottlenecking by a (bulk) *relaxation* process (in contrast to bottlenecking by a third-order recombination process) may be supported by a quantitative analysis. In Sec. V we discuss in more detail the regime where bulk relaxation is the dominant decay process.

To describe the density decays in the doubly-polarized region the data was fit to a simple polynomial expansion in terms of the density: $\dot{n} = C_1 n + C_2 n^2 + C_3 n^3$, and integrating n to obtain the model $n(t)$ and optimize the coefficients C_1, C_2, and C_3 using a nonlinear χ^2 fit of the model $n(t)$ to the observed $n(t)$. Subsequently the coefficients were related to the various decay processes by making use of effective volumes and surfaces. The experimental density n was obtained from the pressure by assuming the gas to be ideal, i.e., $n = p/k_B T$.

Initially we introduced a small amount of helium in the cell, not sufficient to form a saturated helium film. Under this condition we observed the decay to be bottlenecked by a first-order process (C_1). Subsequently the first order rate was suppressed by adding ^{4}He to the system and the decay became bottlenecked by a "higher-order" mechanism. After adding 56 μmol the suppression effect was saturated and all quantitative experiments were done with a coating of at least that amount. We did not observe an influence of the building up of an H_2 coating

in the cell as reported by Reynolds *et al.*[25] A more quantitative discussion of the results on the first-order relaxation will be postponed until Sec. VI.

Most of the remarks made until now also hold for a system with a ^{3}He-^{4}He mixture coating. Nevertheless we observed a remarkable difference between the pure ^{4}He case and the mixtures. This will also be discussed in Sec. VI, after a more detailed discussion of our method of analysis.

IV. DENSITY DECAY KINETICS

The major contributions to the decay process are described by the following rate equations:

$$\begin{aligned}\dot{a} &= \phi_a/V - a/\tau_T - G_{ab}^{i\,\mathrm{eff}}(a-b) \\ &\quad - G_{ab}^{\mathrm{eff}}(a-b)(a+b) - 2K_{aa}^{\mathrm{eff}}aa - K_{ab}^{\mathrm{eff}}ab\ , \\ \dot{b} &= \phi_b/V - b/\tau_T + G_{ab}^{i\,\mathrm{eff}}(a-b) \\ &\quad + G_{ab}^{\mathrm{eff}}(a-b)(a+b) - K_{ab}^{\mathrm{eff}}ab - 2L_3^{\mathrm{eff}}b^3\ .\end{aligned} \tag{4.1}$$

Here a and b represent the a- and b-state densities, respectively, V is the sample volume; the symbol A will be used for the surface area.

The first terms describe the filling flux of the cell for the two different hyperfine levels (ϕ_a and ϕ_b). We assumed $\phi_a=\phi_b$ although in principle these fluxes may be different if the polarization already develops in the filling tube before the atoms reach the actual cell. The second term represents the thermal escape from the cell with τ_T the characteristic time (see Ref. 31 for a further treatment). For our experimental conditions the B/T ratio of the magnetic field to the temperature is sufficiently large for this term to be negligible. The third term describes the relaxation between the hyperfine levels due to impurity relaxation. It depends on the hydrogen surface coverage σ and is expressed as an effective bulk rate constant

$$G_{ab}^{i\,\mathrm{eff}} = (A/V)G_{ab}^{is}(\sigma/n)\ ,$$

with

$$(\sigma/n) = \Lambda \exp(E_a/k_BT)\ . \tag{4.2}$$

Here $n \equiv a+b$, $\Lambda=(2\pi\hbar^2/mk_BT)^{1/2}$ is the thermal wavelength and E_a is the adsorption energy. The fourth terms of Eq. (4.1) account for magnetic relaxation between a and b hyperfine levels due to dipolar couplings between the H atoms.[16–19] Relaxation processes of this type occur both in the bulk *and* on the surface. The total effective rate constant is given by

$$G_{ab}^{\mathrm{eff}} = (A/V)G_{ab}^{s}(\sigma/n)^2 + G_{ab}^{v}\ . \tag{4.3}$$

Recombination appears through the next three terms of Eq. (4.1). The second-order terms involve processes between surface adsorbed atoms in the hyperfine states $|a\rangle$ and $|b\rangle$. The presence of the surface enables the conservation of energy and momentum in the reaction. The a-b and a-a processes are represented by effective bulk rate constants

$$K_{ab}^{\mathrm{eff}} = (A/V)K_{ab}^{s}(\sigma/n)^2$$

and

$$K_{aa}^{\mathrm{eff}} = (A/V)K_{aa}^{s}(\sigma/n)^2\ . \tag{4.4}$$

Recombination between two b-state atoms is assumed to be negligible ($K_{bb}^{s}\simeq 0$).[19] The last term of Eq. (4.1) is related to the third-order recombination rate constant (K_{bbb}^{eff}): $L_3^{\mathrm{eff}} \equiv 2\theta K_{bbb}^{\mathrm{eff}}$. The proportionality constant θ expresses the total number of b-state atoms that are lost in a K_{bbb} event. The constant θ depends on the fate of the third outgoing atom and ranges typically between 1.8 to 1.9.[20,23] The effective rate K_{bbb}^{eff} is defined by

$$K_{bbb}^{\mathrm{eff}} = K_{bbb}^{v} + (A/V)K_{bbb}^{s}(\sigma/n)^3\ . \tag{4.5}$$

All terms except the last one were taken into consideration in the first analysis of the experiments in I. In retrospect this is in part justified as the gas densities were sufficiently low ($n \lesssim 3\times 10^{17}$ cm^{-3}) to neglect the bulk contribution due to K_{bbb}^{v}. However, the surface contribution competes with the relaxation term G_{ab}^{s}. This point, first realized by Hess *et al.*,[22] in relation with their data, will be discussed in Sec. V.

A complication in the analysis of the decays is the strong inhomogeneity of the magnetic field in the cell region. The density profile of the hydrogen gas in this inhomogeneous field changes as a function of temperature and field. It is determined by the balance of the magnetic field gradient forces and the thermal energy,[31]

$$\begin{aligned}n(\mathbf{r}) &= n_0 \exp\{-\mu_B[B(0)-B(\mathbf{r})]/kT\} \\ &\equiv n_0 C(B,T)\ ,\end{aligned} \tag{4.6}$$

where $\mathbf{r}$ is the position in the magnetic field with respect to the center of the magnet, n_0 the density in the center, and μ_B is the Bohr magneton. It is convenient to express this density profile in terms of a dimensionless compression factor $C(B,T)$.

The magnet employed in the experiments has a parabolic field profile described by the radial component B_ρ and the axial component B_z,

$$\begin{aligned}B_z(z,\rho) &= B_0[1-(z/z_m)^2+\tfrac{1}{2}(\rho/z_m)^2]\ , \\ B_\rho(z,\rho) &= z\rho/z_m^2\ ,\end{aligned} \tag{4.7}$$

with ρ the radial distance and z the axial distance from the center, B_0 the field strength in the center, and $z_m=51$ mm for this particular magnet. In the further analysis the small radial components of the field will be ignored.

For the actual cell, effective volumes (V^{eff}) and surfaces (A^{eff}) are calculated by dividing the cell into four cylindrical sections (see Fig. 1), where each section is treated using the method described in Appendix A. For very low temperatures and/or high magnetic fields the density profile is concentrated near the field center. In the geometry sketched in Fig. 1 this means that only the "pancake" shaped part I contributes to A^{eff} and V^{eff}. For high temperatures and/or low fields the profile extends into the fill tube of the cell as well. The various effective volumes and surfaces used in the analysis of our data are plotted in Fig. 4.

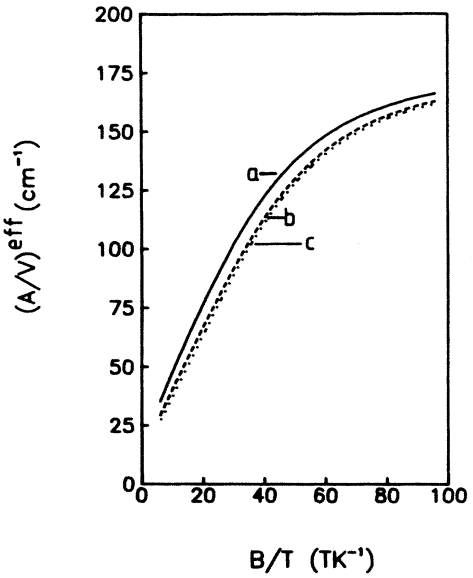

FIG. 4. Effective A/V ratio in the cell of Fig. 1 (see Appendix A for definitions of effective surfaces and volumes): a—$A_1^{\rm eff}/V_1^{\rm eff}$, b—$A_2^{\rm eff}/V_1^{\rm eff}$, c—$A_3^{\rm eff}/V_1^{\rm eff}$.

V. REANALYSIS OF THE DATA: THREE-BODY SURFACE RECOMBINATION

After the observation of three-body surface recombination,[21–23] we decided to reanalyze our data and obtain the three-body surface recombination rate (K_{bbb}^s). A similar reanalysis has been carried out by Bell *et al.*[26] First we will discuss the result of the reanalysis for the data of I for the temperature region where the surface processes are dominant. Then we discuss the results at higher temperature where the decay is dominated by bulk processes and the analysis of I remains unchanged.

The importance of K_{bbb}^s relative to surface relaxation (G_{ab}^s) may be estimated by comparing the measured three-body rate [$L_3^{\rm eff}=2\times10^{-24}$ cm^{4}s^{-1} (Refs. 21–23, and 25)] with the calculated relaxation rate [$G_{ab}^s=3\times10^{-14}$ cm^{2}s^{-1} (Ref. 19)]. The three-body rate is found to become dominant over the two-body relaxation processes for a surface coverage $\sigma > G_{ab}^s/L_3^s \simeq 3\times10^{10}$ cm^{-2}. The typical surface coverage in the decay experiments of I varied from a starting coverage of $\sigma\simeq3\times10^{12}$ cm^{-2} to $\sigma\simeq5\times10^{10}$ cm^{-2} at the end of the recorded decay for temperature range ($T<250$ mK) where the surface processes are dominant. This indicates that three-body recombination must have been the dominant surface decay processes.

The density-decay analysis in I did not provide evidence for a significant third-order coefficient, C_3. As a consequence, in the present analysis we have investigated systematic effects. We found that the data are consistent with a third-order process if we assume a temperature difference ($T-T_0$) to develop between the H gas at temperature T and the copper walls of the sample cell at temperature T_0. This may result from the combined effect of recombination heating and thermal boundary resistance (R_k). To extract an estimate for ($T-T_0$) from our data we use a procedure illustrated in Fig. 5. The decays are well described by a second-order fit ($\dot p=\hat C_1 p+\hat C_2 p^2$) over their whole dynamic range, also in the high-density regions where a temperature gradient is suspected. Note the good quality of the fit. Hence for the present purpose $\hat C_1$ and $\hat C_2$ may be used as fitting parameters to describe the decay. The values of $\hat C_1$ and $\hat C_2$ are readily deduced from the results of I.

A proper description for the decay would be $\dot n=C_1(T)n+C_3(T)n^3$, where C_1 corresponds to first-order surface relaxation and C_3 to the third-order surface recombination process (for the present discussion we will neglect the small contribution of the second-order surface relaxation G_{ab}^s),

$$C_1(T)=2G_{ab}^{is}(A/V)^{\rm eff}\Lambda\exp(E_a/kT)\ ,$$
$$C_3(T)=2\theta K_{bbb}^s(A/V)^{\rm eff}\Lambda^3\exp(3E_a/kT)\ . \tag{5.1}$$

We now use the low-density part of the decay ($\sigma<1\times10^{12}$ cm^{-2}) where $T\simeq T_0$, to determine $C_1(T_0)$ and $C_3(T_0)$. Then from the difference of the observed rate (characterized by $\hat C_1$ and $\hat C_2$) and an extrapolated rate based on $C_1(T_0)$ and $C_3(T_0)$ (dashed line Fig. 5) we can estimate the temperature (T) in the gas. Typically the initial $T-T_0$ is in the order of only 10%, but the change of T during the decay turns out to be sufficient to mimic a second-order behavior.

The importance of $T-T_0$ is determined by the heat production due to recombination in the cell and the dominating thermal boundary (Kapitza) resistance (R_k) (Refs. 13, 32, and 33) between the helium and the copper wall,

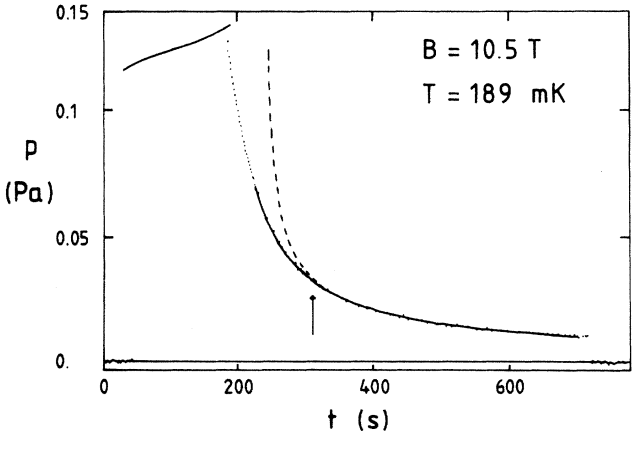

FIG. 5. Estimation of the temperature difference $T-T_0$ in the sample. The solid line is a second-order fit to the data over the whole range of the decay with fitting constants $\hat C_1$ and $\hat C_2$. The dashed line describes the extrapolated decay curve at the temperature T_0 based on first- and third-order decay processes as obtained from the part of the decay where $\sigma<1\times10^{12}$ cm^{-2} (indicated by the arrow). From the difference of the extrapolated curve and the observed decay ΔT can be estimated.

$$T - T_0 \equiv R_k Q = R_k D \dot{n} V^{\text{eff}} , \quad (5.2)$$

where Q is the produced heat, $D = 3.6 \times 10^{-19}$ J is the recombination energy per atom, and V^{eff} is the effective volume where the recombination is taking place. The estimated R_k on the basis of Eq. (5.2) is a factor 4 lower than literature values for the Kapitza resistance[33] between the helium film and the copper surface (the Kapton surface of the pressure gauge is not contributing to A). The Kapitza resistance between the hydrogen gas and the helium surface is apparently even lower than the helium-copper resistance.

The Kapton surface of the pressure gauge is not directly coupled to the cell body, and one may expect that the surface temperature is much higher than the helium-covered copper parts in the cell. An estimate of the thermal conductivity of the helium film, the Kapton and the Au layer of the electrodes of the gauge, show that the average thermal gradient is smaller than $\simeq 5$ mK and that this temperature gradient results in an error of at most 10% in the three-body surface recombination (L^s).

Thus the picture emerges that the hydrogen gas and the helium film are at a temperature T, significantly higher than that of the copper cell wall for which the cell temperature is measured. Since the surface coverage σ depends exponentially on the temperature of the *helium* surface, and since this temperature depends on a power n (the source of the heating), the experimentally observed decay rates for fixed T_0 can acquire a different dependence on n, as $T \to T_0$ as n decays to zero. This problem has also been recently observed and corrected for in the study of the adsorption energy by Godfried *et al.*[34]

Once aware of the thermal problems for the decays with $T < 250$ mK, we reanalyzed the decays always using the same surface coverage at the starting point of the fit independent of the temperature ($\sigma = 1 \times 10^{12}$ cm^2). The typical decay rate $\dot{n} < 1.2 \times 10^{14}$ cm^{-3}s^{-1} implies a released recombination heat $D < 1.7$ μW and the estimated thermal gradient is less than 1.3 mK, much less than the temperature gradients in the analysis of I. We stress the point that although this procedure is well justified in retrospect, the absence of gas temperature data prevents an *ab initio* preference for the present analysis over the analysis in I.

For high temperature (i.e., when $2G_{ab}^v > L_3^{\text{eff}} n$; for $n = 1 \times 10^{17}$ cm^{-3} this is typically fulfilled when $T > 250$ mK) the three-body surface recombination can be neglected. It is sufficient in that case to analyze the decay using $\dot{n} = C_1 n + C_2 n^2$ for modeling the decay, as was done in I. The first-order coefficient provides information on the thermal escape and on the remaining first-order surface (impurity) relaxation. The second-order coefficient describes the nuclear relaxation in the gas phase,

$$C_1 = 2G_{ab}^{is}(A/V)^{\text{eff}}(\sigma/n) , \qquad C_2 = 2G_{ab}^v . \quad (5.3)$$

VI. RESULTS

Figures 6 and 7 show our results for the first-order coefficients. In Fig. 6 the extracted effective first-order relaxation rate $[G_{ab}^{i\,\text{eff}}/(A/V)]$ is plotted as function of $1/T$ at 8 T for different amounts of helium in the cell. This shows qualitatively the suppression of the surface relaxation as a function of the film thickness. It is difficult to make a quantitative estimate of the film thickness based on the amount of helium used. The geometric area of the cell is $\simeq 25$ cm^2, but the different parts are at different temperatures. We estimate from the amounts of hydrogen that were fluxed into the cell, that the H_2 coverage building up during the run is < 30 Å, thus not enough to explain the suppression of the first-order term.

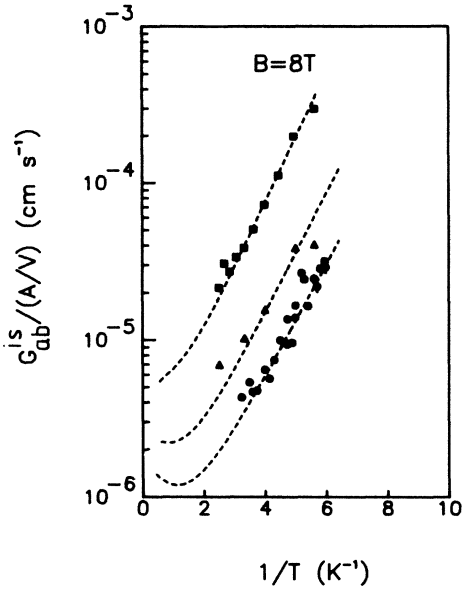

FIG. 6. Temperature dependence of first-order relaxation G_{ab}^{is} for several ^{4}He film thicknesses in the cell. The dashed lines are based on the model of Statt *et al.* (Ref. 25) with a distribution of 66-Å Fe spheres and 10-ppm Fe impurities and film thicknesses: $d = 300$, 250, and 175 Å for 56.1 (●), 39.3 (▲), and 16.8 (■) μmol ^{4}He in the cell, respectively.

Statt *et al.*[25] calculated the surface impurity relaxation induced by a distribution of Fe clusters in the copper of the cell wall. The resulting expression for the G^i depends exponentially on the film thickness d and the surface coverage σ. The dashed line in Fig. 6 is the calculated G^i on the basis of the model of Statt *et al.*[25] using a film thickness $d = 300$ Å, $E_a = 1.0$ K, and a distribution for the iron particles corresponding to 66-Å Fe spheres in copper with 10-ppm Fe impurities (the same cluster size as found by Statt *et al.*: 75 Å, for 0.1 at.% Fe in their OFHC copper). The much lower level of iron contamination in our OFHC copper may explain why we did not observe an influence of a H_2 coating under the helium film as was observed by Statt *et al.*[25]

Figure 7 shows the field dependence of the first-order relaxation term at $T = 189$ mK. The dashed line is again based on the model of Statt *et al.*[25] using the same film thickness and Fe distribution as in Fig. 8. The strong suppression of G^i with increasing magnetic field is caused

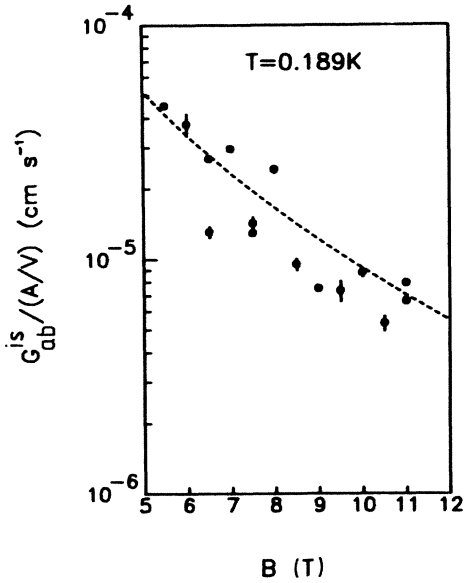

FIG. 7. Field dependence of first-order term at $T=0.189$ K with 56.1 μmol ^{4}He in the cell. The dashed line is based on the same model as in Fig. 6 using the same distribution of Fe impurities and $d=300$ Å. All decay curves are analyzed starting with a surface coverage $\sigma=10^{12}$ cm^{-2}.

by the field dependence of the magnetic transition frequency.[35] The model shows good qualitative agreement with the data both in Figs. 6 and 7. The model does not allow an accurate fit for the cluster size and film thickness independently.

Recently Godfried *et al.*[34] observed an increasing adsorption energy E_a for films thinner than 10 Å. The surface thicknesses used in experiments of Fig. 6 are likely to be much thicker. For the highest coverage (56 μmol ^{4}He in the cell) the surface relaxation is sufficiently suppressed to allow double polarization to build up in the gas.

For data taken at higher temperatures, where surface

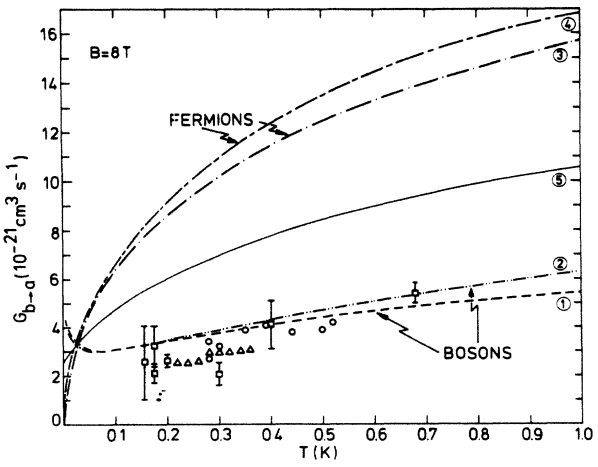

FIG. 8. Nuclear relaxation G_{ab}^{v} in the bulk as function of T (from Ref. 27, data points on ^{3}He films from I are left out).

three-body recombination can be ignored, the analysis of I remains valid. Furthermore, the difference $T-T_0$ is less important under these conditions. The observed second-order rate can be attributed to bulk relaxation G_{ab}^{v} (see Fig. 8). For G_{ab}^{v} the calculated values obtained with different calculation methods agree well with the observed experimental values of all the performed experiments.[5,9,14,15,25] Calculations within the excluded volume approximation and the distorted-wave Born approximation (DWBA) (Refs. 6, 16–19, and 27) give results that agree very well with each other (see Fig. 8). The theoretical temperature and field dependence is well described by the fitting formula obtained by van den Eijnde *et al.*;[36]

$$G_{ab}^{v}=(0.633T^{1/2}+0.757\Delta E_{ab}T^{-1/2})\times10^{-27}(1+\delta/B)^2\ \mathrm{m^3\,s^{-1}}\ , \tag{6.1}$$

with

$$\delta/B=[(g_e\mu_B)/(g_n\mu_n)]\epsilon \simeq[a/(2g_n\mu_n)]1/B\simeq16.68/B$$

and ΔE_{ab} is the energy difference between hyperfine states a and b.

In I decay rates on ^{3}He-^{4}He mixtures (helium added in a ratio ^{3}He:^{4}He of 4:2) were also reported. The adsorption energy of ^{3}He is much lower than on ^{4}He [for ^{3}He $E_a\simeq0.3$–0.42 K (Refs. 10 and 13)]. Consequently the region where surface processes dominate the decay start at a much lower temperature than for ^{4}He surfaces ($T<150$ mK). Nevertheless, the observed rates in I are lower than the estimated value on the basis of the surface coverage σ and the observed surface rates on ^{4}He. This was explained by noting the dependence of G_{ab}^{s} on the angle Ω between the magnetic field and the surface normal as pointed out by Lagendijk,[16]

$$G_{ab}^{s}=G_{s,0}(T)\sin^2(2\Omega)+G_{s,2}(T)\sin^2\Omega(1+\cos^2\Omega)\ . \tag{6.2}$$

This dependence originates from the anisotropy of the dipole-dipole coupling between the spin moments. For $\Omega=0^0$ the rate constant is fully suppressed. However, as argued by Ahn *et al.*[19] the surface is *not* atomically flat and G_{ab}^{s} should be averaged over the surface roughness. As a result the effective G_{ab}^{s} is considerably suppressed for surfaces oriented perpendicular to the magnetic field. Recently Reynolds *et al.*[25] studied the influence of this anisotropy on the NMR transition frequency of the adsorbed atoms and found evidence for the angle dependence of this interaction. In retrospect the suppression of the surface rates as quoted in I can be explained by assuming a temperature difference $T-T_0$. Using the same Kapitza resistance as observed in section on ^{4}He surfaces in our system, the temperature difference becomes $T-T_0\simeq15$ mK for $T_0=80$ mK. Therefore we excluded the measurements on ^{3}He for $T<150$ mK from Fig. 8.

The results for the third-order term are presented in Figs. 9 and 10. In Fig. 9 the effective third-order rate is plotted as function of $1/T$. The slope is consistent with $E_a=1.0$ K and the intercept gives $L_3^s=1.5(2)\times10^{-24}$ cm^{4}s^{-1}. This is in good agreement with the observed value of Hess and co-workers[21–23] when taking into account $\theta=1.9$. The results for the field dependence of the

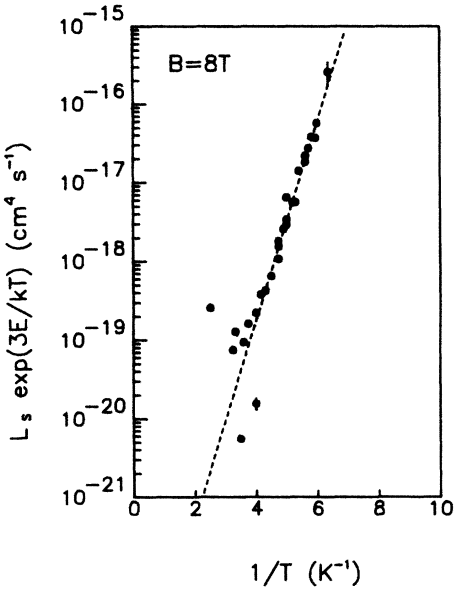

FIG. 9. Temperature dependence of the surface three-body recombination at $B=8$ T. The dashed line is a fit to the data for $1/T>4$ K^{-1}, with $E=1.0$ K and $L_3^s=1.5(2)\times10^{-24}$ cm^{4}s^{-1}.

three-body surface recombination are shown in Fig. 10. A fit to these data, for comparison, using the same fit function as Bell *et al.*,[23] gives

$$L_3^s(B)=L_3^s e^{\eta(B-8.0)}$$

with (6.3)

$$\eta=-0.07(2)\ .$$

This is in good agreement with the values obtained by

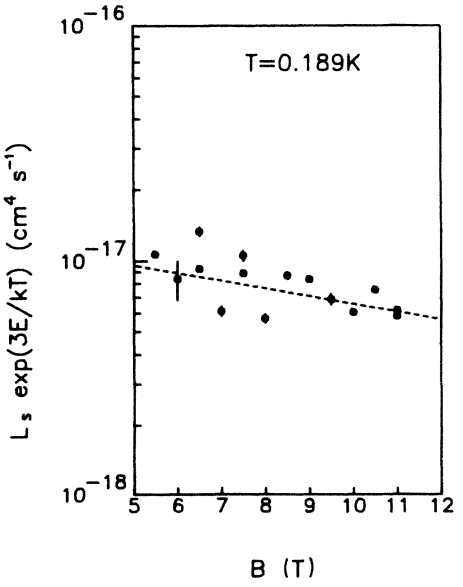

FIG. 10. Field dependence of surface three-body recombination at $T=189$ mK. The dashed line is the fit to the data [see Eq. (6.3)].

Hess and co-workers[21–23] [$\eta=-0.06(2)$] and by Statt and co-workers.[25] Although the decrease of the third-order rate with growing field agrees with other experimental data,[22,23] a disagreement exists with the calculations of de Goey *et al.*[37] These calculations are based on the three-body dipolar recombination mechanism as proposed by Kagan *et al.*,[7,8] the same process thought to be responsible for three-body recombination in the bulk at much higher densities. The calculated K_{bbb}^s (6.5×10^{-26} cm^{4}s^{-1}) is smaller than the observed one ($K_{bbb}^s=L_3^s/2\theta=5.3\times10^{-25}$ cm^{4}s^{-1}, with $\theta=1.9$) and has the opposite field dependence. In principle K_{bbb}^s is also anisotropic, but this effect is much weaker than that of the dipolar relaxation discussed earlier. Comparing theory with experiment, it appears that no theory is available that describes the available experimental three-body rate to a satisfactory level.

By analyzing the data with *only* first- and second-order processes, as was done in the preceding discussion, we have neglected the remaining small contribution from the second-order surface relaxation (G_{ab}^s). On the bases of the observed surface relaxation[25] and the theoretical value[16–19] we estimate an effective rate of $\langle G_{ab}^s=5\times10^{14}$ cm^{-2}s^{-1} in our cell and for the dynamic range of our decays at most effectively a 10% influence on the three-body term L^s.

Analyzing the first part of the decay, when the gas is building up doubly polarization, one can extract the absolute values of K_{aa} and K_{ab}. However, since the average of these rates has already been measured in H↓, it is sufficient to measure the ratio $\gamma=K_{aa}/K_{ab}$. This ratio γ can be obtained by a very simple method. When the system is at very low density ($n\simeq10^{16}$ cm^{-3}) the relaxation ($G_{ab}^{\rm eff}$) in H↓↑ is slow and also three-body recombination on the surface ($L_3^{\rm eff}$) can be ignored. The initial buildup of H↓↑ can then be studied without having to take into account the relaxation (see Fig. 3). The ratio of the initial density and the final density in the double-polarized state is completely determined by the ratio γ. This is easily verified by integrating the rate equations

$$\begin{aligned}\dot a&=-2K_{aa}^{\rm eff}a^2-K_{ab}^{\rm eff}ab\ ,\\ \dot b&=-K_{ab}^{\rm eff}ab\ .\end{aligned}\tag{6.4}$$

One obtains the ratio of the final densities in terms of the initial densities and γ,

$$\begin{aligned}&n(t=\infty)/n(t=0)\\&\quad=\{1+(2\gamma-1)[a(t=0)/b(t=0)]\}^{-1/(2\gamma-1)}\ .\end{aligned}\tag{6.5}$$

An intrinsic uncertainty of this method is the assumption for the initial polarization. Since the experiments are done at low density, it is likely that the buildup of H↓↑ during the filling stage is negligible and that $a(t=0)=b(t=0)$. The experimentally observed ratio was $\gamma=2.23(0.25)$ for temperatures of $T=225$, 250, and 300 mK.

Experiments by Yurke *et al.*[14] made use of an rf field to saturate the initial polarization and to obtain a well-

defined initial condition. Also ESR techniques were used[25] to study this ratio. The results of these measurements are compiled in Fig. 11. The value of γ ranges between 2.2–3.8. The temperature dependence of γ expresses the difference in temperature dependence of K_{aa} and K_{ab}. From the currently available data the detailed temperature dependence of γ is not clear.

Finally we estimate the polarization in our samples. Since at the time of the measurements we did not have a method at our disposal to directly measure the degree of polarization we can only estimate the final polarization in the sample using the model equations and using the measured decay constants. In subsequent experiments ESR techniques were introduced for this purpose by van Yperen *et al.*[15] and in much detail by Reynolds *et al.*[25] while Yurke *et al.*[14] used NMR. In I the influence of L_3^s was not included in the estimate of the polarization. It can be shown that the equilibrium degree of polarization in a sample where three-body terms are important, approaches a density-dependent equilibrium value,[20]

$$a/b = G_{ab}^{\rm eff}/(K_{ab}^{\rm eff} - G_{ab}^{\rm eff} - L_3^{\rm eff} b) \simeq G_{ab}^s/[K_{ab}^s - G_{ab}^s - L_3^s(\sigma/n)b] \,. \quad (6.6)$$

Using $L_3^s = 2\times10^{-24}$ cm^{4}s^{-1} this results in a maximum polarization of $a/b = 99.9\%$ at $B = 8$ T, $T = 225$ mK, and $n = 5\times10^{15}$ cm^{-3}. The presence of a three-body term decreases the polarization, since it forms an extra mechanism to deplete the b state relative to the a state. If the polarization is small ($a/b \simeq 1$), one has to include other decay mechanisms as well (see, e.g., Ref. 20 and 23).

VII. CONCLUSION

The suppression of first-order relaxation is an important step to obtain H↓↑. Careful elimination of (magnetic) surface impurities from the walls of the cell and application of thick helium films seem to be sufficient to suppress the impurity relaxation. The temperature and field dependence of the remaining first-order surface relaxation is described by the model of Statt *et al.*[6]

Analysis of the decay curves at low temperatures, where surface processes are dominant, on the basis of first-order relaxation (G_{ab}^s) and three-body recombination (L_3^s), gives rates that are consistent with more recent measurements.[21–23,25] Also the suppression of L_3^s with an increasing magnetic field is consistent with measurements of Bell *et al.*[22,23]

The apparent second-order behavior used in the previous analysis I was caused by (small) temperature gradients in the gas that change during the decay. These temperature differences also account for the apparent suppression of the surface recombination as reported in I at very low temperature on ^{3}He films.

ACKNOWLEDGMENTS

We thank A. Lagendijk and B. J. Verhaar for a number of stimulating discussions, O. Höpfner for technical support, and J. van Zwol for assistance with the reinterpretation of the data. The financial support of the Stichting voor Fundamenteel Onderzoek der Materie and Department of Energy, Grant No. DE-FG02-85ER45190 is gratefully acknowledged.

APPENDIX A: FIELD AND TEMPERATURE DEPENDENCE OF THE VOLUME-TO-SURFACE RATIO

To illustrate the effect of a density profile on the decay rates, we examine a cylinder with radius R in the parabolic field described by Eq. (4.7). In a small volume element with height dz, surface area dA, and volume dV (see Fig. 12) a decay process (L) of order k with a volume contribution $L^v(B,T)$ and a surface contribution $L^s(B,T)$ can be described by the rate equation,

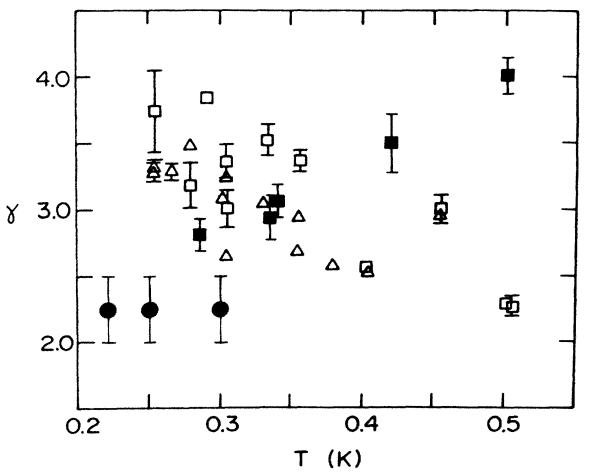

FIG. 11. Compilation of measurements of the ratio $\gamma = K_{aa}/K_{ab}$ [after Silvera and Walraven (Ref. 4)]: (●) Sprik *et al.* (Ref. 5); (■) Yurke *et al.* (Ref. 14), (□△) Statt *et al.* (Ref. 25).

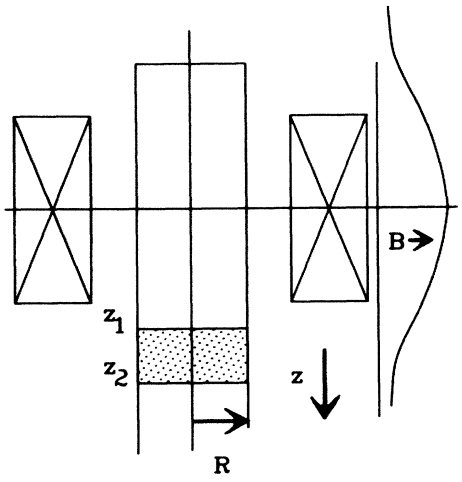

FIG. 12. Part of a cylinder with radius R between z_1 and z_2 with a volume element dV and a surface element dA.

$$d\dot{N} = -dA\, L^s(B,T)(\sigma/n)^k n^k(z) - dV L^v(B,T) n^k(z) . \quad \text{(A1)}$$

In a portion of the cylinder between z_1 and z_2 this results in a rate of the total number of particles given by

$$\dot{N} = \int_{z_1}^{z_2} d\dot{N} = -2\pi R \int_{z_1}^{z_2} L^s(B,T)(\sigma/n)^k n^k dz - \pi R^2 \int_{z_1}^{z_2} L^v(B,T) n^k dz . \quad \text{(A2)}$$

With the use of Eq. (4.6) for the density profile, the total rate becomes

$$\dot{N} = -2\pi R \int_{z_1}^{z_2} L^s(B,T) C^k(B,T) dz\, (\sigma/n)^k n_0^k - \pi R^2 \int_{z_1}^{z_2} L^v(B,T) C^k(B,T) dz\, n_0^k \quad \text{(A3)}$$

and the total number of particles in this section of the cylinder is given by

$$N \simeq \pi R^2 \int_{z_1}^{z_2} n(z) dz = n_0 \pi R^2 \int_{z_1}^{z_2} C(B,T) dz . \quad \text{(A4)}$$

Combining Eqs. (4.6), (A3), and (A4) results in an effective rate equation for the density in the center of the magnet. Since the pressure gauge measures the pressure in the center of the magnet, this equation is needed to model the observed pressure decay. It is also convenient to express the intrinsic field dependence of L^v and L^s in dimensionless constants l^v and l^s with respect to the situation in the field center,

$$L^v(B,T) \equiv l^v(B) L^v(B_0,T) , \quad L^s(B,T) \equiv l^s(B) L^s(B_0,T) . \quad \text{(A5)}$$

Using Eqs. (4.6) and (A3)–(A5) the rate equation for n_0, under uniform thermal conditions in the gas, can be written

$$\dot{n}_0 V_1^{\text{eff}} = -A_{Ls}^{\text{eff}} L^s(B_0,T)(\sigma/n)^k n_0^k - V_{Lv}^{\text{eff}} L^v(B_0,T) n_0^k , \quad \text{(A6)}$$

where the effective volumes and surfaces are defined by

$$V_1^{\text{eff}} = V_{\text{geo}} \left[\int_{z_1}^{z_2} C\, dz/\Delta z \right] , \quad A_{Ls}^{\text{eff}} = A_{\text{geo}} \left[\int_{z_1}^{z_2} l^s C^k dz/\Delta z \right] , \quad V_{Lv}^{\text{eff}} = V_{\text{geo}} \left[\int_{z_1}^{z_2} l^v C^k dz/\Delta z \right] , \quad \text{(A7)}$$

with $V_{\text{geo}} = \pi R^2 \Delta z$, $A_{\text{geo}} = 2\pi R\, \Delta z$ the geometric volume and surface and $\Delta z \equiv z_2 - z_1$ the length of the cylinder. For convenience we have used an abbreviated notation for $l^s(B)$, $l^v(B)$, $C(B,T)$.

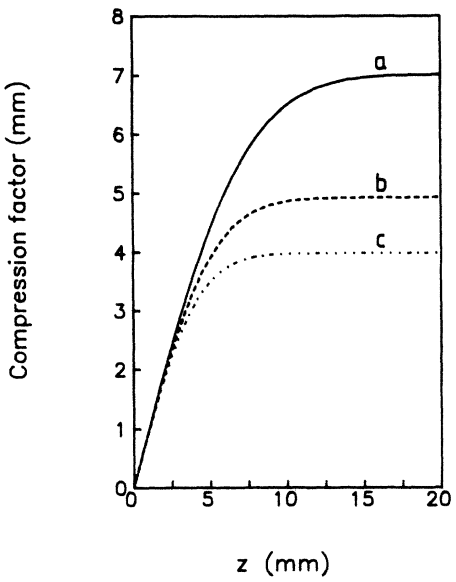

FIG. 13. Compression coefficients for a cylindrical cell in a parabolic field profile. See Appendix A for definitions of compression coefficients: a— $\int_0^z C\, dz$, b— $\int_0^z C^2 dz$, c— $\int_0^z C^3 dz$.

Equation (A6) can be interpreted as an effective rate equation for a field B_0 and a density n_0 in the center. Instead of the geometric volumes and surfaces, one uses effective volumes and surfaces. These effective volumes and surfaces depend on the order of the process (k) *and* on the intrinsic field dependence of the specific decay process [$l^s(B)$ and $l^v(B)$].

In particular, for dipolar relaxation and exchange recombination the intrinsic field dependences are

$$l_{\text{rel}}^s = l_{\text{rel}}^v = [(1+16.68/B)/(1+16.68/B_0)]^2 , \quad l_{\text{rec}}^s = 1/(B/B_0)^2 . \quad \text{(A8)}$$

The corrections due to these intrinsic field dependences is small ($<2\%$). This was verified by numerical evaluation of the effective surfaces in Eq. (A7); the exponential character of the compression factor C dominates the (weaker) intrinsic field dependences. Thus it is sufficient to use only the compression factor to calculate the effective volumes and areas for a particular decay process of order k,

$$V_k^{\text{eff}} = V_{\text{geo}} \left[\int_{z_1}^{z_2} C^k dz/\Delta z \right] , \quad A_k^{\text{eff}} = A_{\text{geo}} \left[\int_{z_1}^{z_2} C^k dz/\Delta z \right] . \quad \text{(A9)}$$

Figure 13 shows the compression factors in a cylinder for decay processes of order k.

*Present address: Philips Medical Systems, Best, The Netherlands.

[1]I. F. Silvera, Physica **109&110B**, 1499 (1982).

[2]J. T. M. Walraven, Physica **126B**, 176 (1984).

[3]T. J. Greytak and D. Kleppner, *New Trends in Atomic Physics,* edited by G. Grynberg and R. Stora (Elsevier, Les Houches, 1984), Vol. II, p. 1125.

[4]I. F. Silvera and J. T. M. Walraven, Prog. Low Temp. Phys. **10**, 139 (1986) (to be published).

[5]R. Sprik, J. T. M. Walraven, G. H. van Yperen, and I. F. Silvera, Phys. Rev. Lett. **49**, 153 (1982).

[6]B. W. Statt and A. J. Berlinsky, Phys. Rev. Lett. **45**, 2105 (1980).

[7]Yu. Kagan, I. A. Vartanyantz, and G. V. Shlyapnikov, Sov. Phys.—JETP **54**, 590 (1981) [Zh. Eksp. Teor. Fiz. **81**, 1113 (1981)].

[8]Yu. Kagan and G. V. Shlyapnikov, Phys. Lett. **88A**, 356 (1982).

[9]R. W. Cline, T. J. Greytak, and D. Kleppner, Phys. Rev. Lett. **47**, 1195 (1981).

[10]G. H. van Yperen, A. P. M. Matthey, J. T. M. Walraven, and I. F. Silvera, Phys. Rev. Lett. **47**, 800 (1981).

[11]A. P. M. Matthey, J. T. M. Walraven, and I. F. Silvera, Phys. Rev. Lett. **46**, 668 (1981); I. F. Silvera and J. T. M. Walraven, Phys. Rev. Lett. **44**, 164 (1980); J. T. M. Walraven, I. F. Silvera, and A. P. M. Matthey, Phys. Rev. Lett. **45**, 449 (1980).

[12]R. W. Cline, D. A. Smith, T. J. Greytak, and D. Kleppner, Phys. Rev. Lett. **45**, 2117 (1980).

[13]M. Morrow, R. Jochemsen, A. J. Berlinsky, and W. N. Hardy, Phys. Rev. Lett. **46**, 195 (1981); **47**, 455(E) (1981); R. Jochemsen, M. Morrow, A. J. Berlinsky, and W. N. Hardy, Phys. Rev. Lett. **47**, 852 (1981).

[14]B. R. Johnson, J. S. Denker, N. Bigelow, L. P. Lévy, J. H. Freed, and D. M. Lee, Phys. Rev. Lett. **52**, 1508 (1984); B. Yurke, J. S. Denker, B. R. Johnson, N. Bigelow, L. P. Lévy, D. M. Lee, and J. H. Freed, Phys. Rev. Lett. **50**, 1137 (1983).

[15]G. H. van Yperen, I. F. Silvera, J. T. M. Walraven, J. Berkhout, and J. G. Brisson, Phys. Rev. Lett. **50**, 53 (1983); G. H. van Yperen, J. T. M. Walraven, and I. F. Silvera, Phys. Rev. B **30**, 2386 (1984).

[16]A. Lagendijk, Phys. Rev. B **25**, 2054 (1982).

[17]A. E. Ruckenstein and E. D. Siggia, Phys. Rev. B **25**, 6031 (1982).

[18]B. W. Statt, Phys. Rev. B **25**, 6035 (1982).

[19]R. M. C. Ahn, J. P. H. W. van den Eijnde, C. J. Reuver, B. J. Verhaar, and I. F. Silvera, Phys. Rev. B **26**, 452 (1982); R. M. C. Ahn, J. P. H. W. van den Eijnde, and B. J. Verhaar, Phys. Rev. B **27**, 5424 (1983); J. P. H. W. van den Eijnde, C. J. Reuver, and B. J. Verhaar, Phys. Rev. B **28**, 6309 (1983).

[20]R. Sprik, J. T. M. Walraven, and I. F. Silvera, Phys. Rev. Lett. **51**, 479 (1983); **51**, 942(E) (1983); R. Sprik, J. T. M. Walraven, and I. F. Silvera, Phys. Rev. B **32**, 5668 (1985).

[21]H. F. Hess, D. A. Bell, G. P. Kochanski, R. W. Cline, D. Kleppner, and T. J. Greytak, Phys. Rev. Lett. **51**, 483 (1983).

[22]H. F. Hess, D. A. Bell, G. P. Kochanski, D. Kleppner, and T. J. Greytak, Phys. Rev. Lett. **52**, 1520 (1984).

[23]D. A. Bell, G. P. Kochanski, L. Pollack, H. F. Hess, D. Kleppner, and T. J. Greytak, *Proceedings of the 17th International Conference on Low-Temperature Physics,* edited by U. Eckern, A. Schmid, W. Weber, and H. Wühl (North-Holland, Amsterdam, 1984), p. 449; D. A. Bell, H. F. Hess, G. P. Kochanski, S. Buchman, L. Pollack, Y. M. Xiao, D. Kleppner, and T. J. Greytak (unpublished).

[24]T. Tommila, S. Jaakkola, M. Krusius, K. Salonen, and E. Tjukanov, *Proceedings of the 17th International Conference on Low Temperature Physics,* Ref. 23, p. 453; T. Tommila, S. Jaakkola, M. Krusius, I. Krylov, and E. Tjukanov, Phys. Rev. Lett. **56**, 941 (1986).

[25]M. W. Reynolds, I. Shinkoda, W. N. Hardy, A. J. Berlinsky, F. Bridges, and B. W. Statt, Phys. Rev. B **31**, 7503 (1985); B. W. Statt, W. N. Hardy, A. J. Berlinsky, and E. Klein, J. Low Temp. Phys. **61**, 471 (1985); B. W. Statt, A. J. Berlinsky, and W. N. Hardy, Phys. Rev. B **31**, 3169 (1985).

[26]D. A. Bell, G. P. Kochanski, D. Kleppner, and T. J. Greytak, *Proceedings of the 17th International Conference on Low-Temperature Physics,* Ref. 23, p. 541.

[27]A. Lagendijk, G. H. van Yperen, and J. T. M. Walraven, J. Phys. Lett. **45**, L929 (1984).

[28]Obtained by chemical analysis of our OFHC copper.

[29]L. J. Azevedo, Rev. Sci. Instrum. **54**, 1793 (1983).

[30]J. T. M. Walraven and I. F. Silvera, Rev. Sci. Instrum. **53**, 1167 (1982).

[31]J. T. M. Walraven and I. F. Silvera, Phys. Rev. Lett. **44**, 168 (1980).

[32]K. T. Salonen, I. F. Silvera, J. T. M. Walraven, and G. H. van Yperen, Phys. Rev. B **25**, 6002 (1982); K. Salonen, S. Jaakkola, M. Karhunen, E. Tjukanov, and T. Tommila, *Proceedings of the 17th International Conference on Low-Temperature Physics,* Ref. 23, p. 543.

[33]O. V. Lounasmaa, *Experimental Principles and Methods Below 1 K* (Academic, New York, 1974).

[34]H. P. Godfried, E. R. Eliel, J. G. Brisson, J. D. Gillaspy, C. Mallardeau, J. C. Mester, and I. F. Silvera, Phys. Rev. Lett. **55**, 1311 (1985).

[35]W. N. Hardy (private communication).

[36]J. P. H. W. van den Eijnde, thesis (University of Eindhoven, 1984) (unpublished).

[37]L. P. H. de Goey, J. P. J. Driessen, B. J. Verhaar, and J. T. M. Walraven, Phys. Rev. Lett. **53**, 1919 (1984).